JEE Journal of Ecological Engineering

Journal of Ecological Engineering 2024, 25(8), 300–316
https://doi.org/10.12911/22998993/189946
ISSN 2299–8993, License CC-BY 4.0

Received: 2024.05.28
Accepted: 2024.06.24
Published: 2024.07.01

Acid Modification and Characterization of Rice Straw Biochar and its Potential as Ameliorant for Saline-Sodic Lowland Soil

June Spencer A. Cera[1*], Jocelyn D. Labios[1], Marcial S. Buladaco II[1], Josefina T. Dizon[2]

[1] Division of Soil Science, Agricultural Systems Institute, College of Agriculture and Food Science, University of the Philippines Los Baños, Philippines

[2] College of Public Affairs and Development, University of the Philippines Los Baños, Philippines

* Corresponding author's e-mail: jacera@up.edu.ph

ABSTRACT

The study aimed to characterize the physicochemical properties of acidified biochar derived from rice straw. The characterization provides useful information on the potential use of rice straw biochar to attain optimal outcomes for environmental or agricultural applications. In this study, rice straw biochar was acidified using 0.1 N HCl three times, followed by washing with deionized water twice, air-dried for seven days, and oven-dried at 80 °C for 8 hours. The characterization showed that the physicochemical properties generally reduced after acid modification. The FESEM-EDS revealed no apparent changes in surface morphology, while elements C, Si, O, N, P, K, Mg, S, Na, Cl, and Al were all determined in acidified biochar. The BET showed that acid modification and pulverization caused a decrease in surface area, pore volume, and pore radius. In ATR-FTIR, additional peaks of carbonyl (C = O Stretch) and alkane (C-H Bend) were identified. Furthermore, XRD showed that acidified biochar confirmed the amorphous structure of the material. In the initial assessment, the addition improved the physicochemical properties of saline-sodic soil by decreasing the pH, ESP, and SAR while increasing WSA, CEC and Mg. Given the results, the reduction and improvement in the properties of acidified biochar demonstrate its potential as soil ameliorant for saline-sodic soil.

Keywords: acid modification, rice straw, biochar, amelioration, saline-sodic soils.

INTRODUCTION

Rice (*Oryza sativa*) is a major crop grown in the islands of the Philippines. The country has a total area of 4.80 million hectares (Mha) dedicated to rice production, of which 3.34 Mha is irrigated and 1.46 Mha is non-irrigated [Philippine Rice Research Institute, 2023]. The abundance of rice straw as a by-product can result in agricultural waste [Villegas-Pangga, 2021]. Given this problem, converting the rice straw to biochar can help address the issue of waste disposal.

Biochar is a product of the thermal decomposition of organic biomass under an inert environment [Sakhiya et al., 2020]. There are various modifications that can be done to biochar, such as impregnation or coating, acid or alkaline washing, steam, gas purging, amination, and engineered carbon. In particular, acid modification through washing of biochar with weak or strong acids can introduce changes to its physicochemical properties. Acids such as HCl, H_2SO_4, H_3PO_4, HNO_3, $C_6H_8O_7$, and $C_2H_2O_4$ can be used to acid modify the properties of biochar [Wang and Wang, 2019]. The effects of acid modification include changes in the elemental composition, pH, EC, functional groups, specific surface area, porosity, and adsorption capacity of biochar [Yakout, 2015; Yakout, 2017; Deng et al., 2018; Xiao et al., 2018; Blenis et al., 2023].

The need to acidify the biochar depends on the purpose of utilizing the material. Various studies have suggested the use of acidified biochar in ameliorating problems such as salt-affected soil [Wang et al., 2022], calcareous soil [Sahin et al., 2017], heavy metals in soil [Boguta et al., 2019], including the improvement of the bioavailability of essential nutrient elements [Zhou et al., 2021; Sultan et al., 2020; He et al., 2020].

There have been various studies characterizing the properties of biochars derived from

agricultural waste [Villegas-Pangga, 2021]. However, the characterization of biochar, more so acidified, is still relatively new and requires further understanding to fully harness its potential application in agriculture or environment [Igalavithana et al., 2017].

The problem on saline-sodic soil or salt-affected soil generally affects approximately 33% of all irrigated lands and 20% of the total croplands worldwide [Nachshon, 2018]. In the Philippines, salt-affected soils in general affects 400,000 hectares, this include areas for mangroves, fishponds, and idle lands [Naungayan et al., 2021] Presently, the Bureau of Soils and Water Management (BSWM), a national government agency under the Department of Agriculture (DA), is currently conducting a nationwide soil testing and mapping of salt-affected areas to provide insights of the country's current status [BSWM, 2024].

The effects of salt on the soil physical properties vary depending on the salinity classes. In saline soil with excess soluble salts, the clay fraction is flocculated and has a better stable structure. Additionally, saline soil is comparable to normal soil in terms of water and air permeability. Conversely, sodic soil adversely affects the soil's physical properties through dispersion. It also results in nutrient imbalances such as Ca^{2+} deficiency and toxicity of Na^{+}, CO_3^{2-}, HCO_3^{-}, MoO_4^{2-}, and other trace elements [Choudhary and Kharche, 2018; Shrivastava et al., 2019].

The potential of acidified biochar to ameliorate saline-sodic soil is based on its specific physicochemical properties, particularly the pH and CEC, which induces the dissolution of $CaCO_3$ followed by exchanging Na^{+} adsorbed on the soil colloids with Ca^{2+} and H^{+} [Sadegh-Zadeh et al., 2018]. In addition, the application of acidified biochar could provide Ca^{2+} and Mg^{2+} that can be exchanged with Na^{+} [El-Sharkawy et al., 2022]. Other mechanisms include the promotion of soil water infiltration and inhibition of evaporation leading to reduction of soluble salts [Huang, 2021]. The reduction in pH, O-containing functional groups, and the pore structure and specific surface area of the material could demonstrate its potential in ameliorating saline-sodic soil [Wang et al., 2022]. Other than specific physicochemical properties of saline-sodic soil, acidified biochar was also found to improve the nutrient availability with the addition acidified biochar [Sultan et al., 2020; Zhou et al., 2021]. Similarly, the mechanisms involved in applying acidified biochar were the same in ameliorating saline-alkali soil [Xia et al., 2024].

In other studies, acidified biochar was used to increase the soil pH buffering capacity resulting in resistance of paddy soil to acidification [He et al., 2022]. Similarly, it was found that it reduced the mobility and bioavailability of heavy metals in coal-mining contaminated soil due to improved adsorption and precipitation [Munir et al., 2020]. The application of acidified biochar also used in calcareous soil where it reduced soil pH and increase electrical conductivity, potassium, available phosphorus, copper, iron, and zinc [Hasanpour et al., 2022]

The application of acidified biochar in ameliorating saline-sodic lowland soil is relatively new and require studies to test possible amelioration strategies. Thus, the objective of this current study was to characterize the physicochemical properties of acidified biochar as potential ameliorant for saline-sodic soils.

MATERIALS AND METHODS

Collection of rice straw biomass

The rice straw biomass was collected at the Experimental Station of the Philippine Rice Research Institute (PhilRice) located at the Institute of Plant Breeding Road, Barangay Putho-Tuntungin, Los Baños, Laguna, Philippines, with coordinates at 14°9'31.55"N and 121°15'34.98"E.

Biochar production

Biochar production was conducted at the Agricultural Systems Institute (ASI) Demonstration and Composting Area, Pili Drive, University of the Philippines (UP) Los Baños.

Prior to the pyrolysis, rice straw biomass was cleaned of foreign objects, air dried, and cut into 4–6 cm lengths. The weight of biomass materials pyrolyzed at each run in the biochar-producing stove was 700 grams. Following a modified procedure of Villegas-Pangga (2021), the biomass material was slowly pyrolyzed at a temperature ranging from 300 °C to 650 °C for 45 minutes and immediately drenched with water after charring to avoid contact with air. The process was followed by transferring the produced biochar onto an air-drying net. The biochar was then air-dried for 7 days, pulverized, and passed through 2 mm sieve, oven-dried at 80 °C for 8 hours. The

moisture content was determined using gravimetric method. The dried biochar was referred to as non-acidified biochar.

Acid modification of biochar

The acid modification was done following the procedure of Sadegh-Zadeh et al. (2018) by washing the non-acidified biochar with 0.1 N HCl at a 1:20 ratio (w/v) three times with an interval of 30 min per batch using an improvised filter with a capacity of 200 g of biochar. This was followed by washing with deionized water twice and then air drying for 7 days. Finally, the acidified biochar was oven-dried at 80 °C for 8 hours. Lastly, gravimetric moisture content was determined. The product was then referred to as acidified biochar.

Characterization of the physicochemical properties of biochar

The characterization of the physicochemical properties of the biochar was conducted at ASI Laboratory, UPLB Nanotechnology Laboratory, and ADMATEL DOST, Philippines.

To evaluate the differences between the non-acidified and acidified biochars, 50 g of both biochars were prepared for physicochemical analysis by pulverizing some samples using a mortar and pestle and sieving through a 0.5 mm diameter mesh. The pH of biochar was measured at a ratio of 1:4 (w/v) using a glass electrode pH meter. Electrical conductivity was also measured with a 1:4 (w/v) biochar-to-water suspension, following the method of Amin and Eissa (2017). For the elemental analyses, the procedures were as follows: organic C was determined by the Walkley and Black method; total N by Kjeldahl method; total P by vanadomolybdate method; and total K by flame photometer method. The elements Ca and Mg were analyzed using NH_4OAc extraction and EDTA titration method, while trace elements Zn and Cu were determined by an atomic absorption spectrometer (AAS). The Fe and Mn were determined by inductive coupled plasma optical emission spectroscopy (ICP-OES) (Shimadzu ICPE-9000).

The surface morphology of acidified and non-acidified biochar was imaged using a field-emission scanning electron microscope (FESEM) with energy dispersive X-ray spectroscopy (EDS) point analysis (Dual Beam Helios Nanolab 600i). Three micrographs were taken at 1000x, 5000x, and 10000× magnifications. In the EDS, two scan points were taken to determine the elemental composition of non-acidified and acidified biochar.

The surface area, pore radius, and pore size were analyzed by multipoint Brunauer-Emmett-Teller (BET) (Quanta Chrome Nova e2200) automated nitrogen multilayer physisorption system. The samples for BET analysis were prepared thoroughly by mixing and oven drying for five hours at 300 °C to remove strongly bound surface water and residual adsorbed gases. The samples were cooled down below 80 °C before unloading the degasser and reweighing to obtain the dry, outgassed weight. The pore size analysis generates an automated 21-adsorption and 20-desorption multipoint BET plot.

Different functional groups or compounds on the non-acidified and acidified biochar were also determined by Attenuated Total Reflectance (ATR) (Perkin Elmer Fourier Transform Infrared Spectrometer) at a range of 4000–600 cm^{-1}. The crystallinity of non-acidified and acidified biochar was also determined using an X-ray Diffractometer (Shimadzu LabX XRD-6100) at 2θ range of 3º to 90º with a scan speed of 1º min^{-1} and a step size of 0.02º. The result was analyzed using X'Pert HighScore by striping k-alpha, Rietveld refining, peak scanning, and matching with ICDD reference.

Initial assessment of acidified biochar efficacy in lowland saline-sodic soil

To test the potential of acidified biochar, a 45-day pot incubation experiment was conducted using a saline-sodic soil obtained from Navotas, Balayan, Batangas (13°55'52.28" N, 120°42'51.04" E). The acidified biochar was applied at a rate of 2.5% w/w into a two-kilogram air-dried soil. A control and a gypsum treatment were also included to benchmark the amelioration capacity of the acidified biochar. The soil was thoroughly mixed by tightly tying up the bags and shaking and mixing the soil to evenly distribute the ameliorants. After mixing, the soil and treatments were transferred to polyethylene pots with a diameter of 15 cm and a height of 12 cm. The incubation experiment consisted of three treatments with three replications arranged in a completely randomized design (CRD) inside a screenhouse. Soil samples were collected at the end of the 45-day experiment. The soil properties associated to salinity (pH, EC, CEC, Na, Ca, and Mg content) were analyzed in the laboratory following standard protocols. In addition, the water

stable aggregate (WSA) was analyzed using wet-sieving method. Exchangeable sodium percentage (ESP) and sodium adsorption ratio (SAR) was calculated by the equations below:

$$ESP = \frac{[Na^+]}{CEC} \times 100 \quad (1)$$

$$SAR = \frac{[Na^+]}{\sqrt{\frac{[Ca^{2+}+Mg^{2+}]}{2}}} \times 100 \quad (2)$$

The data gathered from the initial assessment were analyzed using STAR 2.0.1 (Statistical Tool for Agricultural Research) and R-packages 1.5. The data were described as mean ± standard deviation. Statistically analyzed using one-way analysis of variance (ANOVA) to test the differences among the treatment means at a 5% level of significance. Tukey's honest significant difference (HSD) was used to compare significant treatment means.

RESULTS AND DISCUSSION

Physical and chemical properties of biochar

The chemical properties of the acidified and non-acidified biochar are presented in Table 1. The pH of acidified biochar decreased to 4.27 as a result of the acid modification process. The result was lower than that of non-acidified biochar, which was found to have a pH level of 9.79. According to other reports, the temperature during pyrolysis directly influences the pH of biochar, which is said to increase as the amount of heat increases [Weber and Quicker, 2018; Li et al., 2019]. However, the pH drastically decreases due to the acid modification, which may be attributed to the removal of minerals [Jiang et al., 2018; Deng et al., 2018]. Additionally, the study of Wu et al. (2019), using HCl in the modification process resulted in a drop in pH in the biochar due to complexation and an increase in oxygen functional groups. In the result of FTIR (Figure 5b), carbonyl and an additional peak of alkane peaked after the acid modification.

Table 1. Some physical and chemical properties of non-acidified and acidified rice straw biochar

Analysis	Non-acidified biochar	Acidified biochar
Moisture content, %	14.59	14.46
pH	9.79	4.27
Electrical conductivity, dS m^{-1}	5.37	0.356
Organic carbon, %	15.44	14.91
Nitrogen, %	0.82	0.73
Phosphorus, %	0.85	0.45
Potassium, %	3.25	0.23
Calcium, %	0.4	0.13
Magnesium, %	0.31	0.09
Zinc, mg·kg^{-1}	116.75	113.25
Copper, mg·kg^{-1}	15	20.5
Iron, mg·kg^{-1}	697.29	1685.48
Manganese, mg·kg^{-1}	160.05	274.20

A decrease in electrical conductivity after acid modification was also be noted, with values of 5.37 dS m^{-1} for non-acidified biochar and 0.356 dS m^{-1} for acidified biochar. The EC of biochar is another parameter that is said to be influenced by temperature and heating rates during pyrolysis [Nanda et al., 2015]. The amounts of K, Ca, and Mg in the biochar were higher in non-acidified biochar compared to acidified biochar, which may explain the high EC value [Limwikran et al., 2018]. Additionally, the mineral and ash content may have been removed due to the acid modification process, contributing to low electrical conductivity [Deng et al., 2018]. The OC of the acidified material also reduced, but only for 3%, a less decrease compared with other properties of acidified biochar.

In terms of selected elements, the N, P, K, Ca, Mg, and Zn contents also decreased, which may have been lost during acid modification. A slight decrease from 0.82% to 0.73% was observed on N. Similarly, Zn reduced from 116.75 mg·kg^{-1} to 113.25 mg·kg^{-1}. Apparently, significantly lower values were determined on P, K, Ca, and Mg. The value of P decreased from 0.85 mg kg^{-1} to 0.45 mg·kg^{-1}, this is 47% reduction after acid modification. A lower value was determined on K, which reduced by 93% with its value from 3.25% to 0.23%. The amounts of Ca and Mg also reduced by 67.5% and 71% from their values from 0.4% to 0.13% for calcium and from 0.31% to 0.09% for magnesium. Loss of nutrients in the biochar was also reported in the study of Xiao et al. (2018), which resulted from the demineralization effect of acid hydrolysis. Additionally, the solubility of elements may have also contributed to the decrease of the elements [Wu et al., 2015]. Conversely, Cu, Fe, and Mn increased after acid modification. The Cu content increased from 15 mg·kg^{-1} to 20.5 mg·kg^{-1}, while Fe content increased from 697.29 mg·kg^{-1} to 1685.48 mg·kg^{-1}. Meanwhile, the Mn content increased from 160.05 mg·kg^{-1} to 274.20 mg·kg^{-1}. The increase of Cu, Fe, and Mn was in contrast with the

study of Sahin et al. (2017) and Wang et al. (2018). The increased of the trace elements could be attributed to external factor due to possible contamination especially during drying after the acid modification, which exposes the acidified biochar from various metal sources. However, this requires further study to determine what causes the higher Cu, Fe, and Mn content in acidified biochar.

Surface morphology of biochar

The result of FESEM of non-acidified and acidified biochar reveals that there are differences in the structures of non-acidified and acidified biochar (Figures 1 and Figure 2). The surface structure of acidified biochar revealed that it is porous and has fissures and slits on the surface. This may have resulted from thermal decomposition of volatile matter originating inside the vascular structure of the plant rather than the acid modification process [Rout et al., 2016].

Factors that influence the morphological structure of biochar include temperature, residence time, and biomass [Tan et al., 2017]. Modifications to the biochar can also alter its surface morphology [Blenis et al., 2023]. In this study, acid modification was done by washing the rice straw biochar with 0.1 N HCl. However, through visual inspection, there were no apparent changes in the surface structure of the biochar after acid modification.

Elemental composition of biochar

The EDS analysis of non-acidified and acidified biochar reveals that Si and O dominated the elemental composition of both non-acidified and acidified biochar. In non-acidified biochar, Si obtained a 55.8 wt% in Spectrum 1 (Figure 3a) and 35.1 wt% in Spectrum 2 (Figure 3b). Similarly, acidified biochar also obtained a high wt% of Si. In Spectrum 1 (Figure 4a), Si has a 38.1 wt% and 25.2 wt% in Spectrum 2 (Figure 4b). The presence of Si in both non-acidified and acidified biochar indicates that both materials are Si-rich and could be attributed to the Si accumulation of rice from the soil [Rao and Susmitha, 2017].

Similarly, O is also shown to be consistently high in both non-acidified and acidified biochar. In non-acidified biochar, O was found to be 38.3 wt% in Spectrum 1 (Figure 3a) and 55.1 wt% in Spectrum 2 (Figure 3b). In acidified biochar, the value was determined to be 59.1 wt% in Spectrum 1 (Figure 4a) and 66.2 wt% in Spectrum 2 (Figure 4b). Thus, indicating that both non-acidified and acidified biochar were oxygen-rich. The presence of O can be attributed to the oxygen-containing functional groups that have been formed during the pyrolysis [Tan et al., 2017], and acid modification as confirmed in the ATR-FTIR analysis (Figure 5).

The presence of C was also observed from all scan points for both non-acidified and acidified biochar. However, the quantification was not indicated in the report. Nonetheless, it can be noted that biochar, in general, is a carbon-rich material [Wang and Wang, 2019]. In Table 1, the amount of C in non-acidified biochar is 15.44%, while in acidified biochar the value is 14.91%. In similar studies, Tan et al. (2017) and Xi et al. (2020) reported a C value of 40 wt% from their EDS spectra of biochar derived from rice straw.

There were many other elements observed to be present in both non-acidified and acidified biochar. The elements K, Cl, P, S, Mg, and Na were observed in non-acidified biochar (Figure 3), while N, K, Mg, Na, Al, Cl, and S were determined in acidified biochar (Figure 4). The presence of these elements indicates that both materials were nutrient-rich [Qian et al., 2016; Xi et al., 2020]. Apparently, absence or presence of elements from the scan points for both materials does not necessarily mean that the element no longer exists, rather it was just not observed in the scan points where the EDS analysis was taken.

Surface area, pore volume, and pore radius of biochar

The physisorption analysis presented in Table 2 reveals that acidified biochar has a lower surface area with 1.508 $m^2 \cdot g^{-1}$ compared to non-acidified biochar with 8.719 $m^2 \cdot g^{-1}$. The decrease in surface area was 82.70%, which can be attributed to acid modification. Furthermore, the adsorption and desorption analysis noted a decrease in pore volume and pore radius. In adsorption, the pore volume was found to be less in acidified biochar with only 0.003 $cc \cdot g^{-1}$ compared to non-acidified with 0.012 $cc \cdot g^{-1}$. A similar result was found for the pore volume for desorption, with 0.006 $cc \cdot g^{-1}$ for acidified biochar and 0.007 $cc \cdot g^{-1}$ for non-acidified biochar. The pore radius of non-acidified biochar in desorption also obtained a lower value of only 15.332 Å compared to non-acidified biochar with 154.918 Å. The result revealed that the acid modification process reduced the surface

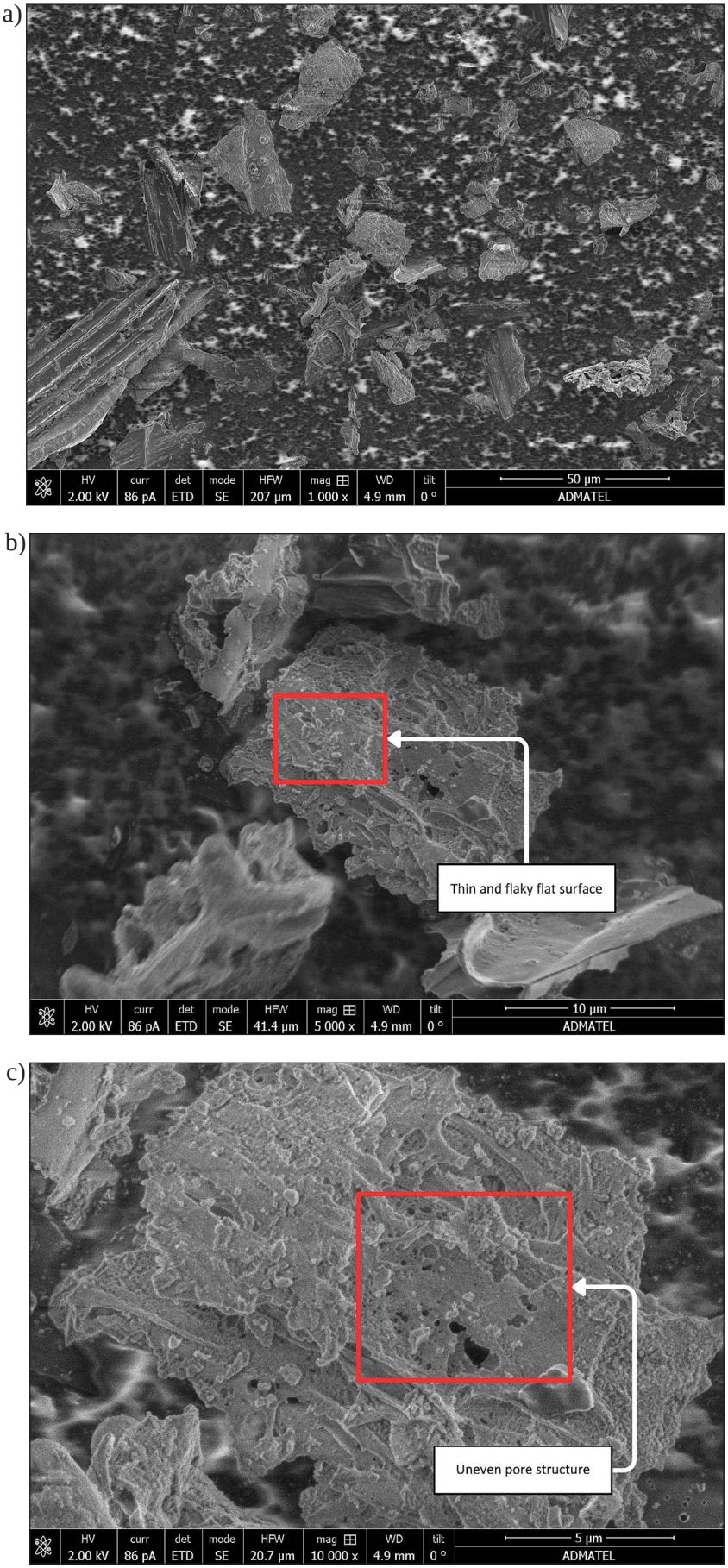

Figure 1. Surface morphology of non-acidified biochar: (a) 1000×, (b) 5000×, and (c) 10000× magnifications

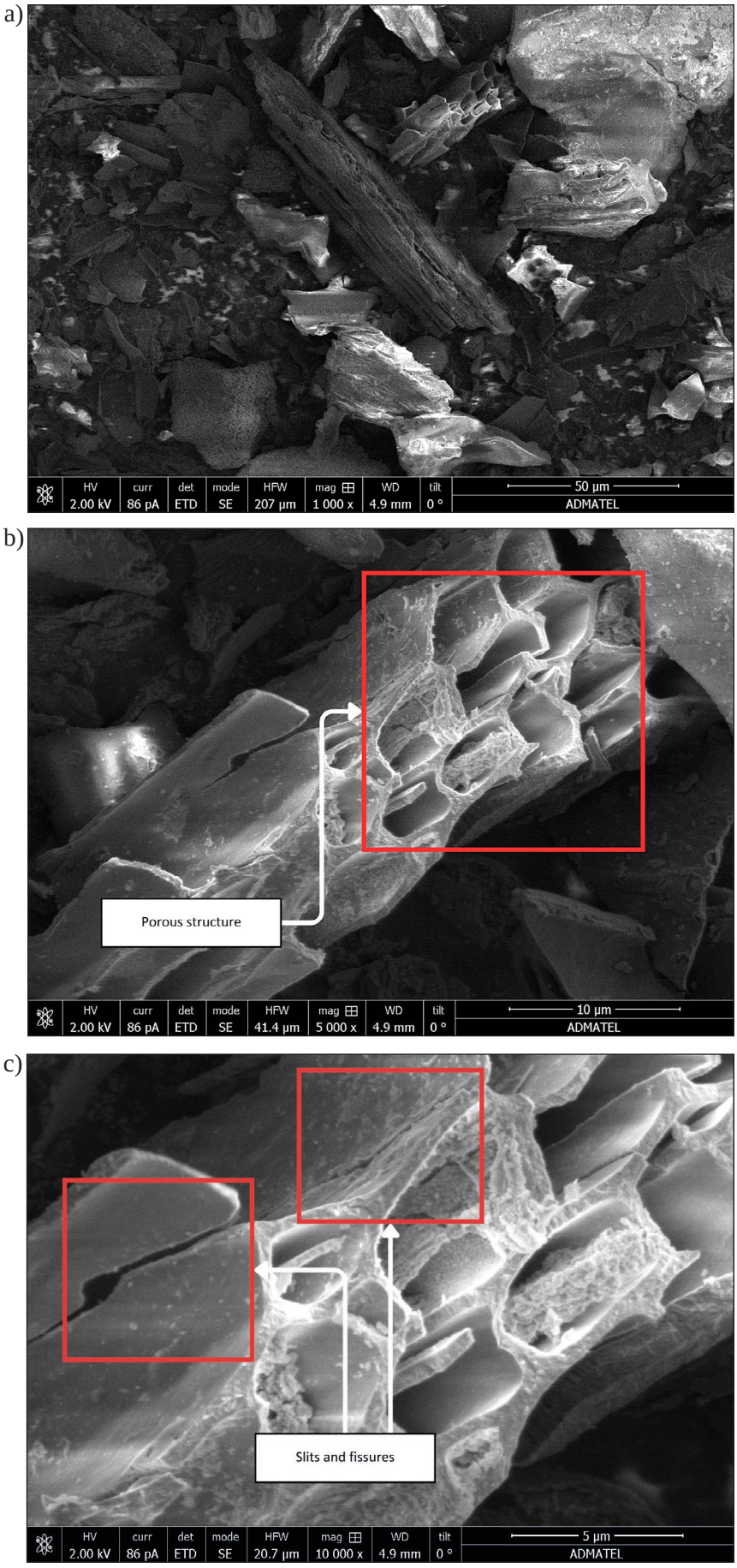

Figure 2. Surface morphology of acidified biochar: (a) 1000×, (b) 5000×, and (c) 10000× magnifications

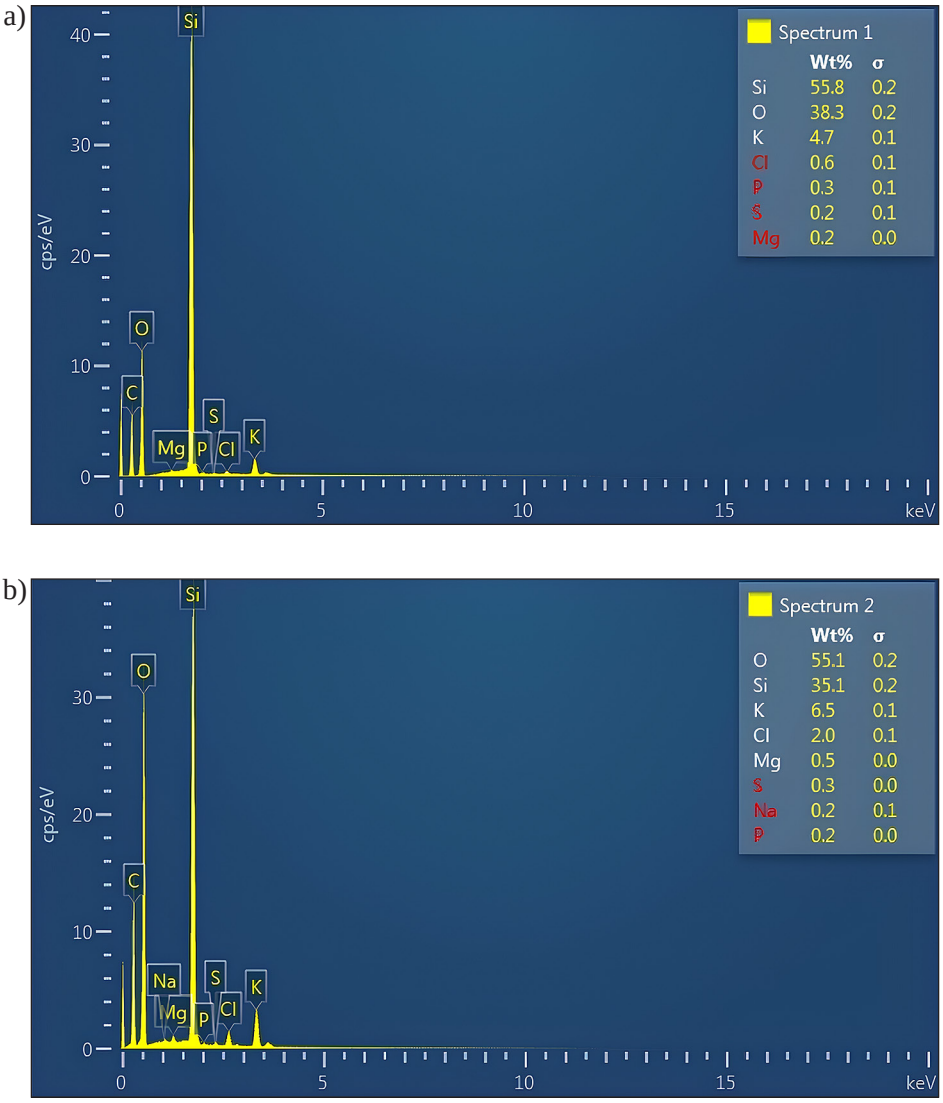

Figure 3. Elemental composition of non-acidified biochar: (a) spectrum 1, (b) spectrum 2

area and pore volume of the biochar. However, the result is in contrast with the study of Wang et al. (2018) and Tong et al. (2016). The acid modification may cause a decrease in surface area through the breaking of the pore structure of the biochar [Panwar and Pawar, 2020]. In a similar study, pulverization of non-acidified and acidified biochar during production resulted in a decrease in surface area and destruction of porosity [Zhang et al., 2016].

There are other factors that may have contributed to the low surface area and pore volume of both biochars. According to Sakhiya et al. (2020), increased reaction temperature and heating rate can result in the reduction of surface area through the melting of cell structure. In addition, it can also result in condensation or devolatilization, destroying the porous structure and clogging pores. The sintering effect followed by shrinking and realignment of the structure of biochar can also lead to the reduction of pore volume and mean size [Angin and Şensöz, 2014].

Functional groups and compounds of biochar

The results of ATR-FTIR analysis presented in Figure 5 reveal different functional groups and compounds. On non-acidified biochar (Figure 5a), a peak at 3378.57 cm^{-1} was determined to be an O-H stretching vibration, indicating the existence of -OH groups (Hydroxyl). The stretching vibration was also found to be present on acidified biochar (Figure 5b) at 3357.14 cm^{-1}, which similarly implies an O-H stretch of OH groups [Behazin et al., 2016]. A similar result was also reported in the study of Tan et al. (2019), where OH groups were also found on the surface of biochar derived from rice straw. The importance of OH groups on

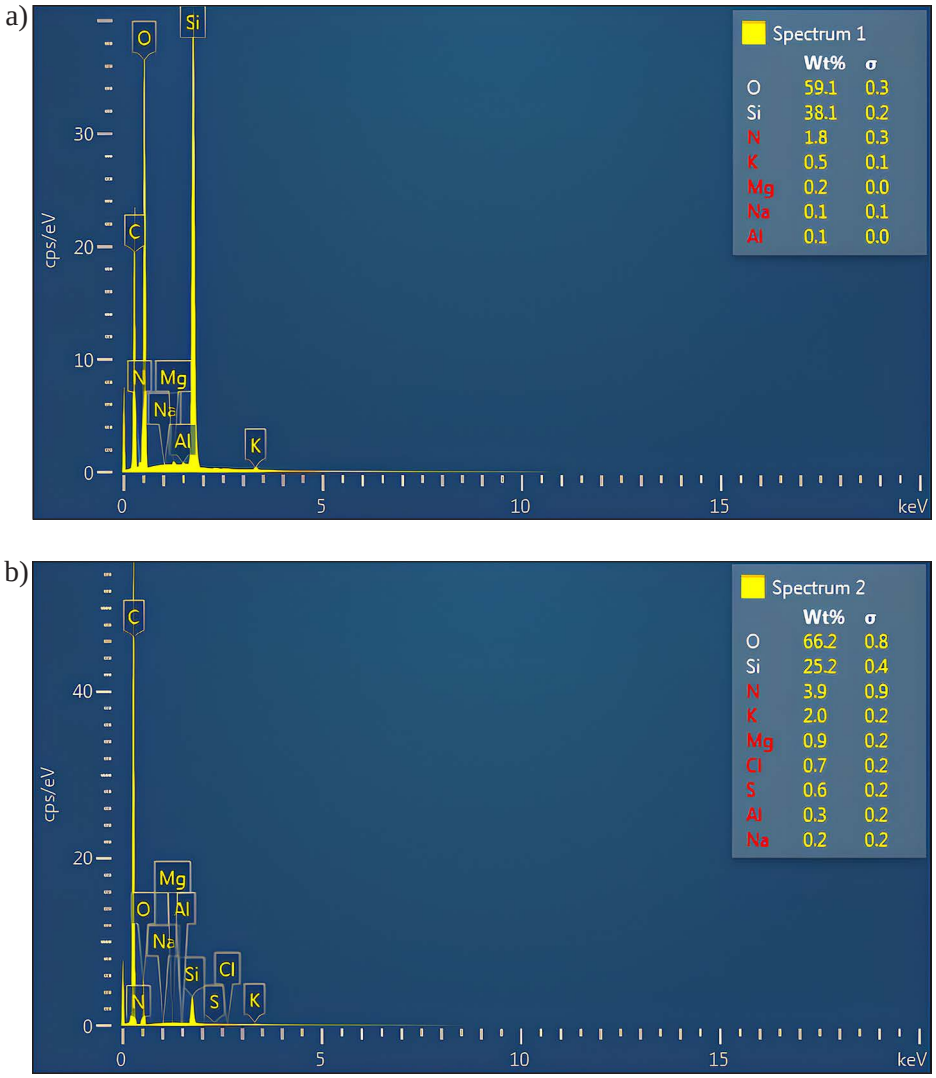

Figure 4. Elemental composition of acidified biochar: (a) spectrum 1, (b) spectrum 2

Table 2. Surface area, pore volume, and pore radius of non-acidified and acidified biochar

Biochar	Surface area ($m^2 \cdot g^{-1}$)	Adsorption		Desorption	
		Pore volume ($cc \cdot g^{-1}$)	Pore radius (å)	Pore volume ($cc \cdot g^{-1}$)	Pore radius (å)
Non-acidified biochar	8.719	0.012	24.820	0.007	154.918
Acidified biochar	1.508	0.003	28.834	0.006	15.332

biochar is said to be the determinant of its negative surface charge, which is affected by increasing temperature [Tan et al., 2020].

The stretch of C-H bond on the surface of non-acidified and acidified biochar at the same frequency of 2925.00 cm^{-1} indicates the presence of alkane on their surfaces [Behazin et al., 2016]. The same stretch of C-H bond at 2920 cm^{-1} was reported by Hu et al. (2022) on the surface of rice straw biochar. Furthermore, C-H bending was observed at 1381.14 cm^{-1} for non-acidified biochar, and 1436.36 cm^{-1} and 1377.57 cm^{-1} for acidified biochar.

According to Biswas et al. (2018), alkanes, together with many other compounds, form during pyrolysis of hemicellulose and cellulose in the feedstock. However, the additional peak of alkane at 1436.36 cm^{-1} on acidified biochar may have been induced by acid modification. A similar result was obtained by Meri et al. (2018), where C-H bending was also determined on biochar treated with HCl.

Noticeably, C = O stretch was determined only on acidified biochar at 1696.81 cm^{-1}, which consisted of carbonyl groups [Behazin et al., 2016].

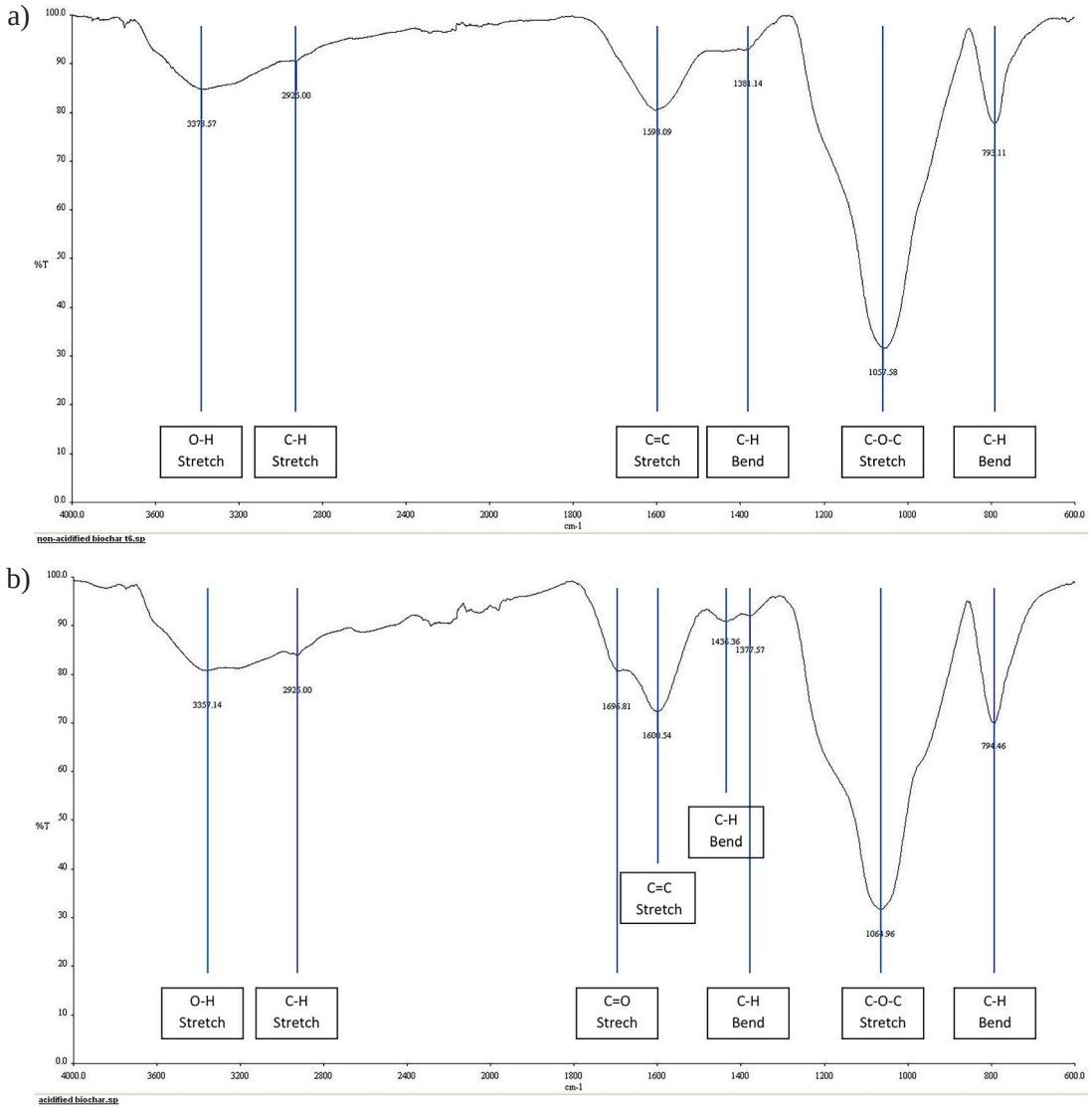

Figure 5. Functional groups of (a) non-acidified biochar and (b) acidified biochar

In the study of Yakout et al. (2015), various acids were used to modify rice straw biochar, which led to the identification of carbonyl. However, the presence of C = O stretching was also determined on rice straw biochar [Ngo et al., 2021] and raw rice straw biomass [Sheng et al., 2014], which explains that carbonyl groups were already present before pyrolysis and even acid modification. The presence of carbonyl may have been a part of the rice straw. Ngo et al. (2021) stated that carbonyl is present in side chains of the lignin structure. Sheng et al. (2014) indicated that it is a usual marker for hemicellulose. However, since it is only found in acidified biochar, acid modification may have increased the presence of carbonyl in the material. Tong et al. (2016) also reported that HCl acid washing on biochar can alter the surface of the material resulting in the determination of carbonyl, carboxyl, and ether.

Stretching of C = C of aromatic compounds was determined on non-acidified and acidified biochar at 1598.09 cm^{-1} and 1600.54 cm^{-1}, respectively, while bending of C-H of aromatic compounds was respectively determined at 793.11 cm^{-1} and 794.46 cm^{-1} of non-acidified and acidified biochar. The presence of aromatic C = C and C–H was also determined by Ngo et al. (2021) on thermally decomposed rice straw. According to Roy et al. (2019), the production of biochar derived from plant material has a high content of aromatic C, which provides the material's resistance and stability against microbial decomposition.

Stretching of C-O-C indicating the existence of ether on non-acidified and acidified biochar was also determined at 1057.58 cm^{-1} and 1064.96 cm^{-1}, respectively. The C-O-C was also determined by Haitao et al. (2017) in the same standard group frequency of 1310–1000 cm^{-1} of

rice straw biochar, confirming its existence on the biochar's surface.

The presence of the identified functional groups is important to various soil properties such as ion adsorption [Yang et al., 2019], anion and cation exchange capacity [Shaaban et al., 2013], pH [Wu et al., 2019], aggregation [Duan et al., 2021], and water holding capacity [Suliman et al., 2017].

Amorphous phase of biochar

The X-ray diffraction results presented in Figures 6 were determined in 2θ and an angle range of 0–90˚. In non-acidified biochar (Figure 6a), amorphous organic compounds represented the peak at $2\theta = 21.1426$ and d = 4.19876. The peak was determined to be graphitized carbon [Wang et al., 2021], as it is observed to have a narrow and sharp diffraction [Wang and Wang, 2019]. Qian and Chen (2013) also reported a similar diffraction peak on rice straw biochar at $2\theta = 15°$ to 30°, which was determined to be amorphous organic compounds (graphitized carbon). No other peaks were found on the diffraction pattern of non-acidified biochar. Various factors may be attributed to the diffraction patterns of biochar, such as temperature [Biswas et al., 2022], material biomass [Pariyar et al., 2020], and modification [Komnitsas and Zaharaki, 2016]. In the study of Qian and Chen (2013), the increased temperature applied to rice straw biochar results in the development of peaks. The temperature applied to the rice straw biochar was 300 °C to 650 °C; however, no apparent peaks were determined at this range. The lack of peaks may also be attributed to the process done during pyrolysis, where the produced biochar was drenched with water to halt the pyrolysis and prevent contact with air. In the study of Xiao et al. (2014), peaks of rice straw-derived biochar at different temperatures were all lost after washing it with water. Thus, the developed crystalline structures during pyrolysis may have been lost during the process.

In Figure 6b, acidified biochar generally has a similar diffraction pattern to non-acidified biochar (Figure 6a). The diffraction at $2\theta = 21.3509$ and d = 4.16170 Å implies amorphous organic compounds of the material under the peak range of $2\theta = 15°$ to 30° [Qian and Chen, 2013]. The diffraction peak was determined to be graphitized carbon by having a narrow and sharp diffraction [Wang et al., 2021]. An additional peak was observed on acidified biochar at a peak position of $2\theta = 77.0800$. The peak matched the ICDD reference, indicating the presence of Aluminum Oxide (Al_2O_3). The diffraction of Al_2O_3 on the surface of acidified biochar may have increased and become more visible due to the acid modification process.

The Al was also confirmed from the FESEM-EDS analysis, where the element was more observable on the surface of acidified biochar compared to non-acidified biochar. The source of Al in the biochar may be attributed to the rice uptake due to its abundance in the soil [Kusa et al., 2021].

Initial assessment of acidified biochar efficacy in lowland saline-sodic soil

Acidified biochar improved the physicochemical conditions of the saline-sodic coastal lowland rice soil (Table 3). For reference, the result of the initial soil analysis showed a pH of 7.2, 8.7 $dS \cdot m^{-1}$ EC, 77% ESP, 22 $meq \cdot L^{-1}$ SAR, and 1.2% WSA. Furthermore, 28.48 $cmol_c \cdot kg^{-1}$ exchangeable Na^+, 16.57 $cmol_c \cdot kg^{-1}$ exchangeable Ca^{2+}, and 17.01 $cmol_c \cdot kg^{-1}$ exchangeable Mg^{2+} were obtained.

Application of biochar (2.5% w/w) yielded similar results as gypsum. Although, not statistically significant, it reduced soil pH which indicates that acidified biochar can be effective in decreasing the pH of saline-sodic soil. The reduction can be attributed to the acidic property of the acidified biochar, which can be due to the complexation and increase in O-containing functional groups [Wu et al., 2019]. The result coincided with the analysis of pH the acidified biochar presented in Table 1 and functional groups in Figure 5. Similar results were also reported by Ahmed et al. (2021), Yuanchengpeng et al. (2019), Sultan et al. (2020), and Ullah et al. (2022). This finding supports the hypothesis that the acidic property of acidified biochar can decrease soil pH when applied as an ameliorant [Ahmed et al., 2021; Soothar et al., 2021]. On the other hand, gypsum application showed to be almost negligible in decreasing the pH of the soil. In comparison, the addition of acidified biochar showed to have a more reduced soil pH than other ameliorants such as $CaCl_2$, rice husk, cow dung, and their combinations [Khan et al., 2019]. Additionally, the use of pristine biochar derived from alfalfa, walnut-shell, sugarcane-bagasse, and combinations with gypsum and aluminum sulfate were comparably found to have higher result in decreasing soil pH than the present experiment [Noori et al., 2021]. Thus, indicating that acidified biochar may have the potential to further reduce soil pH of saline-sodic soil.

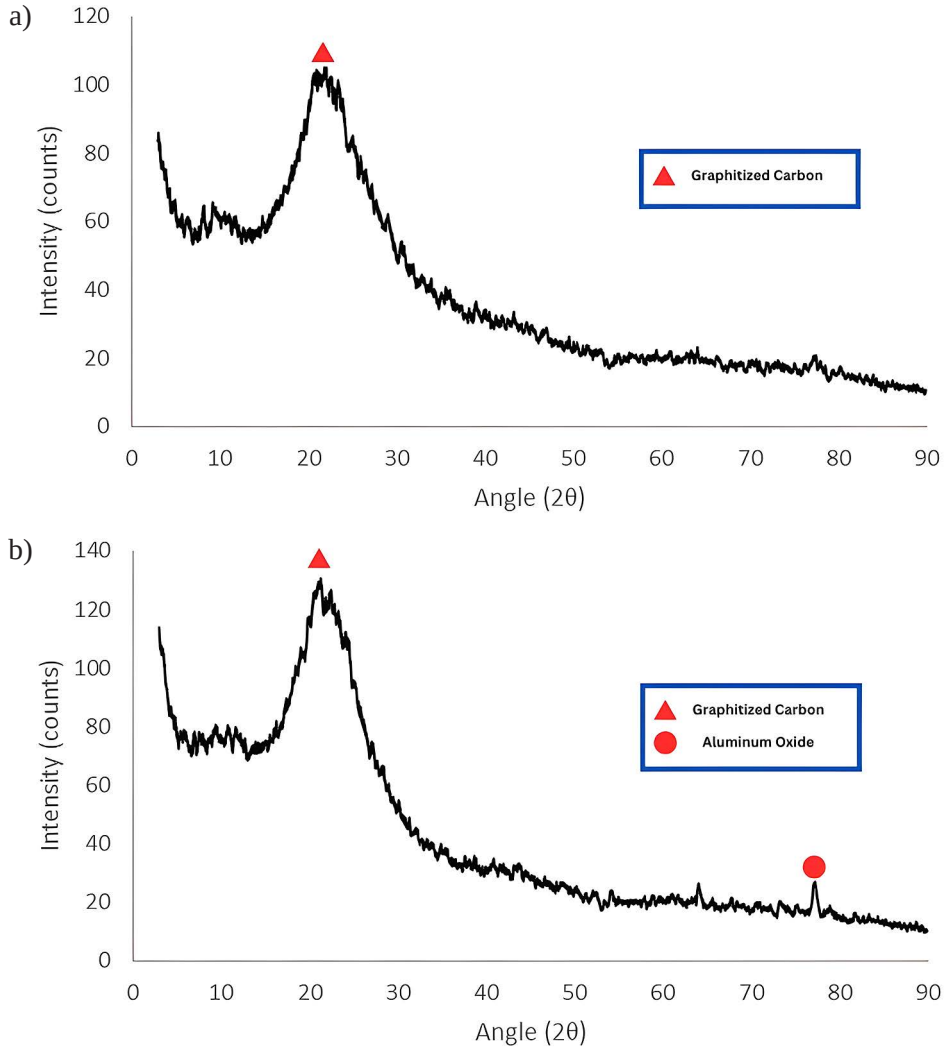

Figure 6. X-ray diffraction pattern of (a) non-acidified biochar and (b) acidified biochar

In contrast, it did not lower soil EC indicating an increase in soluble salts in the soil solution. In Table 1, acidified biochar has low EC while its addition to ameliorated soil resulted in higher electrical conductivity (Table 3). Although not significantly different from the control and gypsum, the higher EC is common with biochar application [Sun et al., 2022; Hafeez et al., 2022]. Similarly, in previous study, other kinds of ameliorants such as the combination of gypsum and aluminum sulfate with biochars were found to yield high ECs [Noori et al., 2021]. However, a reduction in ESP and SAR was observed indicating that basic cations particularly Ca^{2+} and Mg^{2+} were dominantly present than Na^{+} that causes the sodicity problems. Several studies also observed a reduction of ESP and SAR due to the application of acidified biochar [Yuanchengpeng et al., 2019; Bayoumy et al., 2019]. The values obtained in EC, ESP, and SAR were determined to have no significant differences. However, the lower values particularly in ESP and SAR may indicate the possibility of further reduction, which reduces the sodicity of the soil. Relevant to this result, soils ameliorated with acidified biochar and gypsum were found to have lower exchangeable Na than control indicating less adsorbed sodium ions on the exchange sites [Chaganti et al., 2015]. Organic ameliorants

The increase in WSA with the acidified biochar application shows a positive result, indicating an improvement in aggregation in saline-sodic soil. A similar result was obtained from the study of Duan et al. (2021) with the addition of acidified biochar. The aggregation may be attributed to different hypotheses, such as oxygen-containing functional groups [Duan et al., 2021], carbon concentration [Blanco-Canqui, 2018], and harboring of microorganisms [Prakongkep et al., 2020]. Related to this result, the higher presence of oxygen-containing functional groups from the ATR-FTIR

Table 2. Surface area, pore volume, and pore radius of non-acidified and acidified biochar

Biochar	Surface area ($m^2 \cdot g^{-1}$)	Adsorption		Desorption	
		Pore volume ($cc \cdot g^{-1}$)	Pore radius (å)	Pore volume ($cc \cdot g^{-1}$)	Pore radius (å)
Non-acidified biochar	8.719	0.012	24.820	0.007	154.918
Acidified biochar	1.508	0.003	28.834	0.006	15.332

Table 3. Physicochemical properties of ameliorated saline-sodic soil

Treatments	pH	EC	ESP	SAR	WSA	CEC	Na	Ca	Mg
		$dS \cdot m^{-1}$	%	$meq \cdot L^{-1}$	%	$cmol_c \cdot kg^{-1}$	$cmol_c\ kg^{-1}$	$cmol_c \cdot kg^{-1}$	$cmol_c \cdot kg^{-1}$
Control	7.28[a]	7.9[a]	58.76[a]	18.59[a]	1.79[a]	42.13[a]	24.66[a]	18.10[a]	17.06[a]
Acidified biochar	7.15[a]	9.01[a]	53.51[a]	18.38[a]	2.21[a]	45.57[a]	24.30[a]	17.69[a]	17.21[a]
Gypsum	7.27[a]	8.33[a]	53.86[a]	17.65[a]	1.90[a]	43.73[a]	23.56[a]	20.53[a]	15.06[b]
Means with the same letter are not significantly different at 5% level by HSD									

(Figure 5a) and organic C concentration (Table 1) of the acidified biochar could be the reason in higher WSA in ameliorated soil.

It is, however, shown that despite the addition of acidified biochar or gypsum, the WSA is still very low and can be highly attributed to the high levels of exchangeable Na in the soil. With the SAR as an indicator to assess the degree of dispersion, thus WSA, the very high values of SAR correlate with the very low WSA.

The CEC improved with the addition of acidified biochar. Although CEC is already high without any ameliorants and no significant differences were determined, the acidified biochar showed to further improved its value. This result was also reported by Zhou et al. (2021), hypothesized by high CEC of acidified biochar. The observed increase can be due to electrostatic adsorption with the presence of negatively charged functional groups in the biochar forming metal ion complexes in soil [Sun et al., 2022].

In terms of exchangeable cations, a reduction in adsorbed Na and Ca was observed with the addition of acidified biochar, while Mg improved after the incubation period. No significant differences were observed in Na and Ca. However, the decrease, particularly in Na, may further reduce with the addition of acidified biochar. A similar result was determined by He et al. (2020). The reduction could be due to exchanging adsorbed Na^+ with Ca^{2+} and H^+ from the dissolved $CaCO_3$ present in the soil, providing Ca^{2+} and Mg^{2+}, improving soil water infiltration and inhibiting evaporation leading to a decreased amount of soluble salts [Sadegh-Zadeh et al., 2018; El-Sharkawy et al., 2022; Huang, 2021]. On the other hand, adsorbed Mg increased with the addition of acidified biochar, while gypsum was determined to be significantly reduced. The addition of gypsum showed to increase Ca and decrease Na and Mg, indicating that calcium dominated the exchange sites, which can be attributed to the Ca content of gypsum [Abdel-Fattah, 2015]. The use of calcium-rich ameliorants is known to supply Ca^{2+} to replace Na^+ on the exchange sites [Bello et al. 2021]. Other chemicals especially sulfur and sulfuric were also utilized which facilitates dissolution of native calcium minerals in the soil [Chaganti et al., 2015]. However, given the result of the experiment, it could be that Mg is the predominant adsorbed cation rather than Ca which might also explain the result of EDS analysis in Figure 4, where Mg was determined rather than Ca.

CONCLUSIONS

The characterization revealed that acid modification and pulverization led to the reduction and improvement of the properties of acidified biochar. Acid modification showed no apparent effect on the surface morphology of acidified, while EDS showed that both non-acidified and acidified biochar were nutrient-rich materials due to the presence of the majority of macronutrient and micronutrient elements. The surface area, pore volume, and pore radius were reduced in acidified biochar, which were attributed to acid modification and pulverization. In terms of functional groups, carbonyl and additional peaks of alkane were determined on acidified biochar, indicating that oxygen-containing functional groups and compounds improved after acid modification. The

x-ray diffraction showed that acidified biochar was amorphous due to its graphitized carbon property. In the initial assessment, acidified biochar showed the potential to ameliorate saline-sodic lowland soil by decreasing the soil pH, ESP, and SAR, and increasing WSA of the soil. The CEC also improved, decreasing the adsorbed Na and Ca and increasing Mg in the soil. These results indicate the potential of acidified biochar to be used as an ameliorant for saline-sodic soil.

Acknowledgments

The authors would like to express their sincerest gratitude to DOST ASTHRDP-NSC for funding, that made this study possible.

REFERENCES

1. Abdel-Fattah, M.K., Fouda, S., Schmidhalter, U. 2015. Effects of gypsum particle size on reclaiming saline-sodic soils in Egypt. Communication in Soil Science and Plant Analysis, 46(9), 1112–1122. https://doi.org/10.1080/00103624.2015.1018528
2. Ahmed, N., Basit, A., Bashir, S., Bibi, I., Haider, Z., Muhammad Arif Ali, Aslam, Z., Muhammad Aon, Alotaibi, S.S., El-Shehawi, A.M., Tayyaba Samreen, Li, Y. 2021. Effect of acidified biochar on soil phosphorus availability and fertilizer use efficiency of maize (*Zea mays* L.*)*. Journal of King Saud University-Science, 33(8), 101635–101635. https://doi.org/10.1016/j.jksus.2021.101635
3. Angin, D., Şensöz, S. 2014. Effect of pyrolysis temperature on chemical and surface properties of biochar of rapeseed (*Brassica napus* L.). International Journal of Phytoremediation, 16(7–8), 684–693. http://dx.doi.org/10.1080/15226514.2013.856842
4. Amin, A.E.-E.A.Z., Eissa, M.A. 2017. Biochar effects on nitrogen and phosphorus use efficiencies of zucchini plants grown in a calcareous sandy soil. Journal of Soil Science and Plant Nutrition, 17(4), 912–921. https://doi.org/10.4067/s0718-95162017000400006
5. Bayoumy, M.A., Khalifa, T.H.H., Aboelsoud, H.M. 2019. Impact of some organic and inorganic amendments on some soil properties and wheat production under saline-sodic soil. Journal of Soil Sciences and Agricultural Engineering, 10(5), 307–313. https://doi.org/10.21608/JSSAE.2019.43221
6. Behazin, E., Ogunsona, E., Rodriguez-Uribe, A., Mohanty, A.K., Misra, M., Anyia, A.O. 2016. Mechanical, chemical, and physical properties of wood and perennial grass biochars for possible composite application. BioResources, 11(1), 1334–1348.
7. Bello, S.K., Alayafi, A.H., AL-Solaimani, S.G., Abo-Elyousr, K.A.M. 2021. Mitigating Soil Salinity Stress with Gypsum and Bio-Organic Amendments: A Review. Agronomy, 11, 1735. https://doi.org/ 10.3390/agronomy11091735
8. Biswas, B., Singh, R., Kumar, J., Singh, R., Gupta, P., Krishna, B.B., Bhaskar, T. 2018. Pyrolysis behavior of rice straw under carbon dioxide for production of bio-oil. Renewable Energy, 129, 686–694. https://doi.org/10.1016/j.renene.2017.04.048
9. Biswas, B., Balla, P., Krishna, B.B., Adhikari, S., and Bhaskar, T. 2022. Physiochemical characteristics of bio-char derived from pyrolysis of rice straw under different temperatures. Biomass Conversion and Biorefinery, 1-9. https://doi.org/10.1007/s13399-022-03261-y
10. Blanco-Canqui, H. 2019. Biochar and water quality. Journal of Environmental Quality, 48(1), 2–15.
11. Blenis, N., Hue, N., Maaz, T.M., Kantar, M. 2023. Biochar Production, Modification, and Its Uses in Soil Remediation: A Review. Sustainability, 15(4), 3442.
12. Boguta, P., Sokołowska, Z., Skic, K., and Tomczyk, A. 2019. Chemically engineered biochar – Effect of concentration and type of modifier on sorption and structural properties of biochar from wood waste. Fuel, 256, 115893. https://doi.org/10.1016/j.fuel.2019.115893
13. Bureau of Soils and Water Management (BSWM). 2024. National Mapping, Characterization and Development of Spatial Database for the Coastal Areas Affected by Salinity. https://www.bswm.da.gov.ph/program/salinity/
14. Chaganti, V.N., Crohn, D.M., Šimůnek, J. 2015. Leaching and reclamation of a biochar and compost amended saline–sodic soil with moderate SAR reclaimed water. Agricultural Water Management, 158, 255–265. https://doi.org/10.1016/j.agwat.2015.05.016
15. Choudhary, O.P., Kharche, V.K. 2018. Soil salinity and sodicity. Soil science: an introduction, 12, 353–384.
16. Deng, Y., Huang, S., Laird, D.A., Wang, X., Dong, C. 2018. Quantitative mechanisms of cadmium adsorption on rice straw- and swine manure-derived biochars. Environmental Science and Pollution Research, 25, 32418–32432. https://doi.org/10.1007/s11356-018-2991-1
17. Duan, M., Liu, G., Zhou, B., Chen, X., Wang, Q., Zhu, H., Li, Z. 2021. Effects of modified biochar on water and salt distribution and water-stable macro-aggregates in saline alkaline soil. Journal of Soils and Sediments, 21(6), 2192–2202. https://doi.org/10.1007/s11368021-02913-2
18. El-Sharkawy, M., El-Naggar, A.H., Al-Huqail, A.A., Ghoneim, A.M. 2022. Acid-modified biochar impacts on soil properties and biochemical characteristics of crops grown in saline-sodic soils.

Sustainability, 14, 8190. https://doi.org/ 10.3390/ su14138190

19. Hafeez, A., Pan, T., Tian, J., Cai, K. 2022. Modified Biochars and Their Effects on Soil Quality: A Review. Environments 2022(9), 60. https:// doi.org/10.3390/environments9050060
20. Haitao, Z., Shuwen, H., Tianpeng, L., Xu, Y., Zongyu, L., Shengyang, Z., and Peijuan, W. 2017. Effects of preparation conditions and environmental conditions on rice-straw-biochar adsorption of urea. Asia-Pacific Engineering and Technology Conference.
21. Hasanpour, I., Shirvani, M., Hajabbasi, M.A., Majidi, M. M. 2022. Effect of acidic biochars on some chemical properties and nutrient availabilities of calcareous soils. JWSS-Isfahan University of Technology, 26(2), 39–59.
22. He, K., He, G., Wang, C., Zhang, H., Xu, Y., Wang, S., Kong, Y., Zhou, G., and Hu, R. 2020. Biochar amendment ameliorates soil properties and promotes Miscanthus growth in a coastal saline-alkali soil. Applied Soil Ecology, 155, 103674. https://doi.org/10.1016/j.apsoil.2020.103674
23. He, X., Hong, Z.N., Shi, R.Y., Cui, J.Q., Lai, H.W., Lu, H.L., and Xu, R.K. 2022. The effects of H2O2-and HNO3/H2SO4-modified biochars on the resistance of acid paddy soil to acidification. Environmental Pollution, 293, 118588. https://doi.org/10.1016/j.envpol.2021.118588
24. Hu, Y., Li, P.Y., Yang, Y.P., Ling, M., and Li, X.F. 2022. Preparation and Characterization of Biochar from Four Types of Waste Biomass under Matched Conditions. BioResources, 17, 4.
25. Huang, C. 2021. Effects of common biochar and acid-modified biochar on soil water and salt distribution and spinach growth in a tidal flat area. https://doi.org/10.27441/d.cnki.gyzdu.2021.001194
26. Igalavithana, A.D., Mandal, S., Niazi, N.K., Vithanage, M., Parikh, S.J., Mukome, F.N., Rizwan, M., Oleszczuk, P., Al-Wabel, M., Bolan, N., Tsang, D.C.W., Kim. K.H., and Ok, Y.S. 2017. Advances and future directions of biochar characterization methods and applications. Critical Reviews in Environmental Science and Technology, 47(23), 2275–2330.
27. Jiang, B., Lin, Y., and Mbog, J.C. 2018. Biochar derived from swine manure digestate and applied on the removals of heavy metals and antibiotics. Bioresource Technology. https://doi.org/10.1016/j.biortech.2018.08.022
28. Khan, M.Z., Azom, M.G., Sultan, M.T., Mandal, S., Islam, M.A., Khatun, R., Billah, S.M. and Ali, A.H.M.Z. 2019. Amelioration of saline soil by the application of gypsum, calcium chloride, rice husk and cow dung. Journal of Agricultural Chemistry and Environment, 8, 78–91. https://doi.org/10.4236/jacen.2019.82007
29. Komnitsas, K.A., and Zaharaki, D. 2016. Morphology of modified biochar and its potential for phenol removal from aqueous solutions. Frontiers in Environmental Science, 4, 26.
30. Kusa, K., Moriizumi, M., Hobara, S., Kaneko, M., Matsumoto, S., Kasuga, J., and Ae, N. 2021. Mineral weathering and silicon uptake by rice plants promote carbon storage in paddy fields. Soil Science and Plant Nutrition, 67(2), 162–170.
31. Li, S., Harris, S., Anandhi, A., and Chen, G. 2019. Predicting biochar properties and functions based on feedstock and pyrolysis temperature: A review and data syntheses. Journal of Cleaner Production, 215, 809–902. https://doi.org/10.1016/j.jclepro.2019.01.106
32. Limwikran, T., Kheoruenromne, I., Suddhiprakarn, A., Prakongkep, N., and Gilkes, R.J. 2018. Dissolution of K, Ca, and P from biochar grains in tropical soils. Geoderma, 312, 139–150.
33. Meri, N.H., Alias, A.B., Talib, N., Rashid, Z.A., Wan, W.A., and Ghani, A.K. 2018. Effect of chemical washing pre-treatment of empty fruit bunch (EFB) biochar on characterization of hydrogel biochar composite as bioadsorbent. In IOP Conference Series: Materials Science and Engineering, 358 (1), 12–18.
34. Munir, M.A.M., Liu, G., Yousaf, B., Ali, M.U., Abbas, Q., and Ullah, H. 2020. Synergistic effects of biochar and processed fly ash on bioavailability, transformation and accumulation of heavy metals by maize (*Zea mays* L.) in coal-mining contaminated soil. Chemosphere, 240, 124845. https://doi.org/10.1016/j.chemosphere.2019.124845
35. Nachshon, U. 2018. Cropland soil salinization and associated hydrology: Trends, processes and examples. Water, 10(8), 1030.
36. Nanda, S., Dalai, A.K., Berruti, F., and Kozinski, J.A. 2015. Biochar as an Exceptional Bioresource for Energy, Agronomy, Carbon Sequestration, Activated Carbon and Specialty Materials. Waste and Biomass Valorization, 7(2), 201–235. https://doi.org/10.1007/s12649-015-9459-z
37. Naungayan, D.L., Sorsano, J.M., and Farin, E.N. 2021. Effect of soil organic ameliorant s with carbonized rice hull on the growth and yield of shallot onion (*Alliu m ascalonicum* L.) on salt affected soil. Asian J Agric Res, 8(3), 19–28. https://doi.org/10.9734/AJAHR/2021/v8i330117
38. Ngo, T.N.L.T., and Chiang, K.Y. 2021. Co-thermal degradation characteristics of rice straw and sewage sludge. Sustainable Environment Research, 31(1). https://doi.org/10.1186/s42834-021-00096-6
39. Noori, Z., Delavar, M.A., Safari, Y., and Alavi-Siney, S.M. 2021. Reclamation of a calcareous sodic soil with combined amendments: interactive effects of chemical and organic materials on soil chemical properties. Arabian Journal of Geosciences, 14, 1–11. https://doi.org/10.1007/s12517-021-06485-w

40. Panwar, N.L., and Pawar, A. 2020. Influence of activation conditions on the physicochemical properties of activated biochar: a review. Biomass Conversion and Biorefinery, 12, 925–947. https://doi.org/10.1007/s13399-020-00870-3
41. Pariyar, P., Kumari, K., Jain, M.K., and Jadhao, P.S. 2020. Evaluation of change in biochar properties derived from different feedstock and pyrolysis temperature for environmental and agricultural application. Science of the Total Environment, 713, 136433.
42. Philippine Rice Research Institute (PhilRice). 2023. Area harvested. https://www.philrice.gov.ph/ricelytics/harvestareas
43. Prakongkep, N., Gilkes, R., Wisawapipat, W., Leksungnoen, P., Kerdchana, C., Inboonchuay, T., Delbos, E., Strachan, L.J., Ariyasakul, P., Ketdan, C., and Hammecker, C. 2020. Effects of biochar on properties of tropical sandy soils under organic agriculture. Journal of Agricultural Science, 13(1), 1–17.
44. Qian, L., and Chen, B. 2013. Dual role of biochars as adsorbents for aluminum: the effects of oxygen-containing organic components and the scattering of silicate particles. Environmental Science and Technology, 47(15), 8759–8768.
45. Qian, L., Chen, B., and Chen, M. 2016. Novel alleviation mechanisms of aluminum phytotoxicity via released biosilicon from rice straw-derived biochars. Scientific Reports, 6(1), 1–11.
46. Rao, G. B., and Susmitha, P. 2017. Silicon uptake, transportation and accumulation in Rice. Journal of Pharmacognosy and Phytochemistry, 6(6), 290–293.
47. Rout, T., Pradhan, D., Singh, R.K., and Kumari, N. 2016. Exhaustive study of products obtained from coconut shell pyrolysis. Journal of Environmental Chemical Engineering, 4(3), 3696–3705. https://doi.org/10.1016/j.jece.2016.02.024
48. Roy, S., Kumar, U. and Bhattacharyya, P. 2019. Synthesis and characterization of exfoliated biochar from four agricultural feedstock. Environmental and Pollution Research, 26, 7272–7276. https://doi.org/10.1007/s11356-018-04117-7
49. Sadegh-Zadeh, F., Parichehreh, M., Jalili, B., and Bahmanyar, M. A. 2018. Rehabilitation of calcareous saline-sodic soil by means of biochars and acidified biochars. Land Degradation and Development, 29(10), 3262–3271.
50. Sahin, O., Taskin, M.B., Kaya, E.C., Atakol, O.R.H.A.N., Emir, E., Inal, A., and Gunes, A.Y. D.I.N. 2017. Effect of acid modification of biochar on nutrient availability and maize growth in a calcareous soil. Soil Use and Management, 33(3), 447–456. https://doi.org/10.1111/sum.12360
51. Sakhiya, A.K., Anand, A., and Kaushal, P. 2020. Production, activation, and applications of biochar in recent times. Biochar, 2, 253–285. https://doi.org/10.1007/s42773-020-00047-1
52. Shaaban, A., Se, S.M., Mitan, N.M.M., and Dimin, M.F. 2013. Characterization of biochar derived from rubber wood sawdust through slow pyrolysis on surface porosities and functional groups. Procedia Engineering, 68, 365–371.
53. Sheng, J., Ji, D., Yu, F., Cui, L., Zeng, Q., Ai, N., and Ji, J. 2014. Influence of chemical treatment on rice straw pyrolysis by TG-FTIR. Ieri Procedia, 8, 30–34.
54. Shrivastava, M., Kumar, S., Yadav, S., Manasvini., Lal, K. 2019. Deficiency and toxicity of trace elements in salt-affected soil. journal of soil salinity and water quality. Indian Society of Soil Salinity and Water Quality, 11(1), 31–44.
55. Soothar, M.K., Mounkaila Hamani, A.K., Kumar Sootahar, M., Sun, J., Yang, G., Bhatti, S. M., and Traore, A. 2021. Assessment of acidic biochar on the growth, physiology and nutrients uptake of maize (*Zea mays* L.) seedlings under salinity stress. Sustainability, 13(6), 3150. https://doi.org/10.3390/su13063150
56. Suliman, W., Harsh, J.B., Abu-Lail, N.I., Fortuna, A.M., Dallmeyer, I., and Garcia-Pérez, M. 2017. The role of biochar porosity and surface functionality in augmenting hydrologic properties of a sandy soil. Science of the Total Environment, 574, 139–147. https://doi.org/10.1016/j.scitotenv.2016.09.025
57. Sultan, H., Ahmed, N., Mubashir, M., and Danish, S. 2020. Chemical production of acidified activated carbon and its influences on soil fertility comparative to thermo-pyrolyzed biochar. Scientific Reports, 10(1), 595.
58. Sun, Z., Hu, Y., Shi, L., Li, G., Pang, Z.H.E., Liu, S., Chen, Y., and Jia, B. 2022. Effects of biochar on soil chemical properties: A global meta-analysis of agricultural soil. Plant, Soil and Environment, 68(6), 272–289. https://doi.org/10.17221/522/2021-PSE
59. Tan, Z., Zou, J., Zhang, L., and Huang, Q. 2017. Morphology, pore size distribution, and nutrient characteristics in biochars under different pyrolysis temperatures and atmospheres. Journal of Material Cycles and Waste Management, 20(2), 1036–1049. https://doi.org/10.1007/s10163-017-0666-5
60. Tan, G., Liu, Y., and Xiao, D. 2019. Influence of different pyrolysis methods on the sorption property of rice straw biochar. Separation Science and Technology, 54(17), 2773–2782.
61. Tan, Z., Yuan, S., Hong, M., Zhang, L., and Huang, Q. 2020. Mechanism of negative surface charge formation on biochar and its effect on the fixation of soil Cd. Journal of Hazardous Materials, 384, 121370. https://doi.org/10.1016/j.jhazmat.2019.121370
62. Tong, Y., Mayer, B. K., and Mcnamara, P.J. 2016. Triclosan adsorption using wastewater biosolids-derived biochar. Environmental Science: Water Research and Technology, 2(4), 761–768.
63. Ullah, I., Khan, S., Nawab, J., Khan, M.A., and

Jehan, S. 2022. Hardwood modified and unmodified biochar amendments used for saline alkali soil remediation: phosphorus availability and its plant uptake. Arabian Journal of Geosciences, 15(9), 910.

64. Villegas-Pangga, G. 2021. Production and characterization of biochars from slow Pyrolysis of different biomass materials to evaluate properties as soil amendments. Philippine Journal of Science, 150(1), 267–276
65. Wang, T., Wu, J., Zhang, Y., Liu, J., Sui, Z., Zhang, H., Chen, W.Y., Norris, P., and Pan, W. P. 2018. Increasing the chlorine active sites in the micropores of biochar for improved mercury adsorption. Fuel, 229, 60–67. https://doi.org/10.1016/j.fuel.2018.05.028
66. Wang, J., and Wang, S. 2019. Preparation, modification and environmental application of biochar: a review. Journal of Cleaner Production, 227, 1002–1022. https://doi.org/10.1016/j.jclepro.2019.04.282
67. Wang, C., Huang, R., Sun, R., Yang, J., and Sillanpää, M. 2021. A review on persulfates activation by functional biochar for organic contaminants removal: Synthesis, characterizations, radical determination, and mechanism. Journal of Environmental Chemical Engineering, 9(5), 106267.
68. Wang, Z., Pan, X., Kuang, S., Chen, C., Wang, X., Xu, J., Li, X., Li, H., Zhuang, Q., Zhang, F., and Wang, X. 2022. Amelioration of coastal salt-affected soils with biochar, acid modified biochar and wood vinegar: Enhanced nutrient availability and bacterial community modulation. International Journal of Environmental Research and Public Health, 19(12), 7282.
69. Weber, K., and Quicker, P. 2018. Properties of biochar. Fuel, 217, 240–261. https://doi.org/10.1016/j.fuel.2017.12.054
70. Wu, H., Che, X., Ding, Z., Hu, X., Creamer, A.E., Chen, H., and Gao, B. 2015. Release of soluble elements from biochars derived from various biomass feedstocks. Environmental Science and Pollution Research, 23(2), 1905–1915. https://doi.org/10.1007/s11356-015-5451-1
71. Wu, J., Wang, T., Zhang, Y., and Pan, W.P. 2019. The distribution of Pb (II)/Cd (II) adsorption mechanisms on biochars from aqueous solution: considering the increased oxygen functional groups by HCl treatment. Bioresource Technology, 291, 121859.
72. Xi, J., Li, H., Xi, J., Tan, S., Zheng, J., and Tan, Z. 2020. Effect of returning biochar from different pyrolysis temperatures and atmospheres on the growth of leaf-used lettuce. Environmental Science and Pollution Research, 27, 35802–35813. https://doi.org/10.1007/s11356-020-09840-8
73. Xia, X., Riaz, M., Babar, S. Li, Y., Wang, X., Wang, J., and Jiang, C. 2024. Acid-modified cotton straw biochar has instructive for the improvement of saline-alkali soil. J Soils Sediments. https://doi.org/10.1007/s11368-024-03800-2
74. Xiao, X., Chen, B., and Zhu, L. 2014. Transformation, morphology, and dissolution of silicon and carbon in rice straw-derived biochars under different pyrolytic temperatures. Environmental Science and Technology, 48(6), 3411–3419.
75. Xiao, R., Wang, J.J., Li, R., Park, J., Meng, Y., Zhou, B., Pensky, S., and Zhang, Z. 2018. Enhanced sorption of hexavalent chromium [Cr (VI)] from aqueous solutions by diluted sulfuric acid-assisted MgO-coated biochar composite. Chemosphere, 208, 408–416. https://doi.org/10.1016/j.chemosphere.2018.05.175
76. Yakout, S.M. 2015. Monitoring the changes of chemical properties of rice straw–derived biochars modified by different oxidizing agents and their adsorptive performance for organics. Bioremediation Journal, 19(2), 171–182. https://doi.org/10.1080/10889868.2015.1029115
77. Yakout, S.M. 2017. Physicochemical characteristics of biochar produced from rice straw at different pyrolysis temperature for soil amendment and removal of organics. Proceedings of the National Academy of Sciences, India Section A: Physical Sciences, 87(2), 207–214. https://doi.org/10.1007/s40010-017-0343-z
78. Yang, X., Wan, Y., Zheng, Y., He, F., Yu, Z., Huang, J., Wang, H., Ok, Y.S., Jiang, Y., and Gao, B. 2019. Surface functional groups of carbon-based adsorbents and their roles in the removal of heavy metals from aqueous solutions: a critical review. Chemical Engineering Journal, 366, 608–621. https://doi.org/10.1016/j.cej.2019.02.119
79. Yuanchengpeng, Cai, C., and Cuijingwen. 2019. Study on Improvement Effect of Saline-alkali Soil by Cationic Modified Biochar. In IOP Conference Series: Earth and Environmental Science, 310(4), 42–46.
80. Zhang, J., Chen, Q., and You, C. 2016. Biochar effect on water evaporation and hydraulic conductivity in sandy soil. Pedosphere, 26(2), 265–272. https://doi.org/10.1016/s1002-0160(15)60041-8
81. Zhou, Z., Li, Z., Zhang, Z., You, L., Xu, L., Huang, H., Wang, X., Gao, Y., and Cui, X. 2021. Treatment of the saline-alkali soil with acidic corn stalk biochar and its effect on the sorghum yield in western Songnen Plain. Science of The Total Environment, 797, 149190. https://doi.org/10.1016/j.scitotenv.2021.149190